

AperTO - Archivio Istituzionale Open Access dell'Università di Torino

**Effects of the antioxidant moieties of dissolved organic matter on triplet-sensitized phototransformation processes: Implications for the photochemical modeling of sulfadiazine**

**This is the author's manuscript**

*Original Citation:*

*Availability:*

This version is available <http://hdl.handle.net/2318/1687055> since 2019-01-17T12:06:17Z

*Published version:*

DOI:10.1016/j.watres.2017.10.020

*Terms of use:*

Open Access

Anyone can freely access the full text of works made available as "Open Access". Works made available under a Creative Commons license can be used according to the terms and conditions of said license. Use of all other works requires consent of the right holder (author or publisher) if not exempted from copyright protection by the applicable law.

(Article begins on next page)

# **Effects of the antioxidant moieties of dissolved organic matter on triplet-sensitized phototransformation processes: Implications for the photochemical modeling of sulfadiazine**

**Davide Vione,<sup>a,b,\*</sup> Debora Fabbri,<sup>a</sup> Marco Minella,<sup>a</sup> Silvio Canonica<sup>c,\*</sup>**

<sup>a</sup> *Dipartimento di Chimica, Università degli Studi di Torino, Via P. Giuria 5, I-10125 Turin, Italy.*

<sup>b</sup> *Università di Torino, Centro Interdipartimentale NatRisk, Largo Paolo Braccini 2, I-10095 Grugliasco (TO), Italy.*

<sup>c</sup> *Eawag, Swiss Federal Institute of Aquatic Science and Technology, Ueberlandstrasse 133, CH-8600 Dübendorf, Switzerland.*

\* Address correspondence to either author. [davide.vione@unito.it](mailto:davide.vione@unito.it); [silvio.canonica@eawag.ch](mailto:silvio.canonica@eawag.ch)

## ***Abstract***

Previous studies have shown that the photodegradation of some pollutants, induced by the excited triplet states of chromophoric dissolved organic matter (<sup>3</sup>CDOM\*), can be inhibited by back-reduction processes carried out by phenolic antioxidants occurring in dissolved organic matter (DOM). Here, for the first time to our knowledge, we included such an inhibition effect into a photochemical model and applied the model predictions to sulfadiazine (SDZ), a sulfonamide antibiotic that occurs in surface waters in two forms, neutral HSDZ and anionic SDZ<sup>-</sup> (pK<sub>a</sub> = 6.5). The input parameters of the photochemical model were obtained by means of dedicated experiments, which showed that the inhibition effect was more marked for SDZ<sup>-</sup> than for HSDZ. Compared to the behavior of 2,4,6-trimethylphenol, which does not undergo antioxidant inhibition

when irradiated in natural water samples, the back-reduction effect on the degradation of SDZ was proportional to the electron-donating capacity of the DOM. According to the model results, direct photolysis and  $\cdot\text{OH}$  reaction would account for the majority of both HSDZ and  $\text{SDZ}^-$  photodegradation in waters having low dissolved organic carbon ( $\text{DOC} < 1 \text{ mgC L}^{-1}$ ). With higher DOC values ( $> 3\text{-}4 \text{ mgC L}^{-1}$ ) and despite the back-reduction processes, the  $^3\text{CDOM}^*$  reactions are expected to account for the majority of HSDZ phototransformation. In the case of  $\text{SDZ}^-$  at high DOC, most of the photodegradation would be accounted for by direct photolysis. The relative importance of the triplet-sensitized phototransformation of both  $\text{SDZ}^-$  and (most importantly) HSDZ is expected to increase with increasing DOC, even in the presence of back reduction. An increase in water pH, favoring the occurrence of  $\text{SDZ}^-$  with respect to HSDZ, would enhance direct photolysis at the expense of triplet sensitization. SDZ should be fairly photolabile under summertime sunlight, with predicted half-lives ranging from a few days to a couple of months depending on water conditions.

**Keywords:** Antioxidants; Sulfadiazine; Electron Donating Capacity; Dissolved Organic Matter; Environmental Photochemistry.

## 1. Introduction

Sulfadiazine (SDZ) is a sulfonamide antibiotic inhibiting the bacterial enzyme dihydropteroate synthase, involved in the synthesis of folate that is an important growth factor for the bacterial cells (Madigan et al., 2012). SDZ is included in the World Health Organization (WHO) list of essential medicines (WHO, 2017), namely the most important medications needed in a basic health system. It

is used in the treatment of urinary tract infections, toxoplasmosis, malaria, and against bacterial infections that may arise in the HIV disease (NIH, 2017).

SDZ is metabolized in the human body with urinary excretion of the parent compound, together with its hydroxylated, sulfated and glucuronised derivatives (Vree et al., 1995). SDZ is partially removed but not completely eliminated from wastewater in wastewater treatment plants (WWTPs) (Li and Zhang, 2011; Huang et al., 2016). The occurrence of SDZ in wastewater treatment basins and wastewater effluents at  $\mu\text{g L}^{-1}$  levels (Gao et al., 2012; Vosough et al., 2015) has the potential to induce SDZ resistance in bacteria (Yuan et al., 2014). In addition to WWTP effluents, also the use of SDZ in aquaculture and livestock breeding is an important SDZ source to surface waters (Li et al., 2016a; Sun et al., 2016).

Due to the aforementioned sources, SDZ has been detected in surface waters at  $\text{ng L}^{-1}$  to  $\text{sub-}\mu\text{g L}^{-1}$  levels (Chen et al., 2013; Giang et al., 2015; Li et al., 2016b; Sakai et al., 2016). Although not among the most persistent sulfonamide antibiotics, SDZ has a biodegradation half-life in river water of about 20-30 days (Adamek et al., 2016). This compound can also undergo photodegradation by direct and indirect photochemistry (Diaz et al., 2004; Boreen et al., 2005; Bahnmüller et al., 2014), and photodegradation has been shown to affect significantly its overall fate (Giang et al., 2015). Moreover, it has been shown that SDZ biodegradation can be accelerated by SDZ photolysis intermediates (Pan et al., 2014). The direct photodegradation of SDZ has been found to be faster at higher pH (Bian and Zhang, 2016) and to be affected by the formation of complexes with dissolved Fe(III), although the importance of the latter pathway at the Fe(III) levels that naturally occur in surface waters is still uncertain (Zhang and Ma, 2013; Batista et al., 2014). The pH effect on photolysis is likely accounted for by the fact that SDZ is a weak acid with  $\text{pK}_a = 6.5$  (Lin et al., 1997; Sanli et al., 2010). Therefore, the occurrence of both the undissociated form and the anionic one (hereafter HSDZ and  $\text{SDZ}^-$ , respectively) should be taken into account when modeling the environmental fate of SDZ (*vide infra*).

Direct photolysis and indirect photoreactions with  $\bullet\text{OH}$  and the triplet states of chromophoric dissolved organic matter ( $^3\text{CDOM}^*$ ) account for the majority of SDZ phototransformation in most surface-water conditions (Boreen et al., 2005; Bahnmüller et al., 2014). Among these photoreaction pathways, the direct photolysis occurs when a pollutant absorbs sunlight (Boreen et al., 2003). In the case of indirect photochemistry, the irradiation of chromophoric dissolved organic matter (CDOM) mainly yields  $^3\text{CDOM}^*$ ,  $^1\text{O}_2$  and  $\bullet\text{OH}$ . The radical  $\bullet\text{OH}$  is also produced by irradiation of nitrate and nitrite. The radical  $\bullet\text{OH}$  occurs at a higher extent in shallow and low-DOC waters, while the  $^3\text{CDOM}^*$  and  $^1\text{O}_2$  reactions tend to prevail in high-DOC and deep environments (Vione et al., 2014; Cory et al., 2009; Wenk et al., 2013). The photochemical modeling of SDZ phototransformation, which is one of the goals of the present work, is enabled by the literature availability of the direct photolysis quantum yields and of the reaction rate constants with  $\bullet\text{OH}$  and  $^1\text{O}_2$  (Boreen et al., 2005). Moreover, the second-order rate constants for the quenching of the triplet state of 4-carboxybenzophenone ( $^3\text{CBBP}^*$ ) by HSDZ and  $\text{SDZ}^-$  have been measured recently by Li et al. (2015). CBBP is a suitable proxy for CDOM, as there is evidence that the  $^3\text{CBBP}^*$  reactivity is quite close to that of  $^3\text{CDOM}^*$  (Avetta et al., 2016). The triplet quenching rate constants are here assumed to be close to the rate constants of HSDZ/ $\text{SDZ}^-$  transformation induced by  $^3\text{CBBP}^*$  and, therefore, to the rate constants of transformation by  $^3\text{CDOM}^*$ .

The reaction between SDZ and  $^3\text{CDOM}^*$  is not a straightforward process, however, because of the occurrence of back-reduction phenomena (Wenk and Canonica, 2012; Wenk et al., 2015). Indeed, the dissolved organic matter (DOM) that occurs in natural waters comprises both photoactive moieties (CDOM) and antioxidant groups, e.g., phenolic moieties. The  $^3\text{CDOM}^*$  species are oxidants usually involved in one-electron or H-atom abstraction from dissolved substrates (including the xenobiotics), producing oxidized transformation intermediates. The oxidized intermediates can undergo further reactions finally resulting in xenobiotic transformation. In alternative, they could also interact with easily oxidizable DOM moieties to undergo back-

reduction and produce again the original xenobiotic. SDZ is among the xenobiotics that undergo the back-reduction phenomenon, which causes an inhibition of triplet-sensitized degradation (Canonica and Laubscher, 2008; Wenk and Canonica, 2012). Back-reduction processes have been described in the laboratory, and they have the potential to inhibit the phototransformation of compounds such as SDZ in deep and DOM-rich waters.

Deep water columns are out of reach for laboratory experiments, but they are accessible to photochemical modeling (Bodrato and Vione, 2014). To this purpose, this paper has the goal of assessing the impact of back reduction under conditions that are representative of surface waters. For instance, high-DOC conditions would increase both the steady-state [ $^3\text{CDOM}^*$ ] and the back-reduction effect (McNeill and Canonica, 2016), with an overall outcome on the importance of triplet-sensitized phototransformation that is still to be assessed. To do so, however, one needs additional experimental data. The effect of antioxidants on the triplet-sensitized degradation of SDZ is presently available for a single pH value, and with a model sensitizer that is different from 4-carboxybenzophenone. In this paper, we: *(i)* study the back-reduction process for both HSDZ and  $\text{SDZ}^-$  in synthetic solutions; *(ii)* irradiate SDZ in natural water samples to get insight into the antioxidant effect in shallow water; *(iii)* verify that the observed trends can be reproduced by photochemical modeling, and *(iv)* extrapolate the model predictions to deeper water columns. We compare the SDZ results with those obtained with 2,4,6-trimethylphenol (TMP) under similar conditions. TMP is a compound for which photodegradation in natural water is mainly triggered by  $^3\text{CDOM}^*$  (the TMP direct photolysis and reactions with  $\bullet\text{OH}$  and  $^1\text{O}_2$  are only minor processes) (Al Housari et al., 2010; De Laurentiis et al., 2012). Moreover, differently from SDZ, TMP does not undergo back-reduction in the presence of DOM antioxidants (Canonica and Laubscher, 2008; Wenk et al., 2015).

## 2. Experimental section

### 2.1. Reagents and materials

Sulfadiazine (SDZ, purity grade 99%) and 2,2'-azino-bis(3-ethylbenzothiazoline-6-sulfonic acid) diammonium salt (ABTS, 98.0%) were purchased from Sigma, 4-carboxybenzophenone (CBBP, 99%), 4-nitroanisole (97%), pyridine (99%) and NaNO<sub>3</sub> (99%) from Aldrich, phenol (99.5%) and H<sub>3</sub>PO<sub>4</sub> (85%) from Fluka, NaH<sub>2</sub>PO<sub>4</sub>×H<sub>2</sub>O (99%) and Na<sub>2</sub>HPO<sub>4</sub>×2 H<sub>2</sub>O (99.5%) from Merck, 2,4,6-trimethylphenol (TMP, 99%) from EGA-Chemie, and acetonitrile (gradient grade) from Acros Organics. Ultra-pure water (resistivity > 18 MΩ cm, organic carbon < 2 ppb) was provided by a Barnstead Nanopure system.

The surface water samples were collected in the Piedmont region (NW Italy). Grab sampling was carried out with 1 L Pyrex glass bottles, from the shore of four lakes (Avigliana, Maggiore, Candia and Viverone) and two paddy fields (Santhià and San Germano Vercellese). The water samples were transported under refrigeration to the laboratory, vacuum filtered using cellulose acetate filter membranes (Sartorius, 47 mm diameter, 0.45 μm pore size), and stored under refrigeration till use or analysis.

### 2.2. Irradiation experiments

The solutions to be irradiated (20 mL total volume) were introduced in quartz tubes that were then closed with glass stoppers. When required, the pH of the irradiated solutions was adjusted by addition of a phosphate buffer solution (final concentration of phosphate 5 mM). The tubes were placed in a DEMA (Hans Mangel GmbH, Bornheim-Roisdorf, Germany) model 125 merry-go-round photoreactor, equipped with a Heraeus Noblelight TQ718 medium-pressure mercury lamp

operated at 500 W and a borosilicate glass cooling jacket. The used apparatus can irradiate up to nine tubes at the same time. A 0.15 M NaNO<sub>3</sub> solution, passed through a Lauda RK 20 cooling thermostat, was used as a water bath to keep the irradiated tubes at a temperature of 25.0 ± 0.5 °C and to remove lamp radiation of wavelength < 320 nm. The latter condition was employed to minimize the direct photolysis of SDZ. The photolysis of nitrate yields nitrite that absorbs radiation at longer wavelengths (Mack and Bolton, 1999) and might modify the filter transmittance. Therefore, the stability over time of the filter solution was monitored by measuring its transmittance at 360 nm and by checking that it was above 85% for the effective optical path length of ≈3 cm. The irradiation intensity in the quartz tubes was checked by chemical actinometry using an aqueous solution of 4-nitroanisole (5 μM) and pyridine (10 mM) (Dulin and Mill, 1982), and it was estimated to vary by < ±7% over the whole series of irradiation experiments. At scheduled irradiation times, 0.5 mL sample aliquots were withdrawn from each tube, placed in HPLC vials and kept refrigerated until analysis.

### ***2.3. Analytical determinations***

The time trends of SDZ and TMP were monitored by high-performance liquid chromatography with diode-array detection (HPLC-DAD). The used instrument was an Agilent 1100 chromatograph, PC-controlled with a Chromeleon 7 Chromatography Data System software. The column used was a reverse-phase Cosmosil 5 C18-MS-II (100 mm × 3 mm × 5 μm), kept at 25°C in the column oven. SDZ was eluted at 0.7 mL min<sup>-1</sup> flow rate, with a 90% A / 10% B mixture of A = aqueous H<sub>3</sub>PO<sub>4</sub> at pH 2.1 and B = acetonitrile, with retention time ( $t_R$ ) of 2.7 min and detection at 267 nm. TMP was eluted with 50% A / 50% B, with  $t_R$  = 3.0 min and detection at 210 nm.

In most experiments, the time trend of TMP and of SDZ was fitted with an exponential function of the form  $C_t = C_o e^{-kt}$ , where  $C_t$  is the substrate concentration at the time  $t$ ,  $C_o$  the initial



concentration, and  $k$  the pseudo-first order degradation rate constant. The initial transformation rate is  $R = k C_o$ . In some experiments, i.e., in the case of SDZ irradiated in natural water, the time trend was observed to deviate from a pure pseudo-first order kinetics. In these cases, data fitting was performed using an exponential trend with a residual,  $C_t = a e^{-kt} + b$ , where  $a$  and  $b$  are free-floating fit parameters and the initial transformation rate is given by  $R = k C_o a (a + b)^{-1}$ . Such a deviation from pseudo-first order is expected to arise from aging of the irradiated solutions, possibly due to CDOM photobleaching, reversible formation of photolysis products, as well as changes in the antioxidant capacity of the solutions.

The natural water samples were characterized for the absorption spectra and the content of dissolved organic and inorganic carbon (DOC and DIC, respectively). The DOC and DIC values were measured by catalytic wet oxidation and by acidification plus gas stripping, respectively, followed by non-dispersive IR detection. The used instrument was a Shimadzu TOC-VCSH analyzer, equipped with an ASI-V autosampler. Further details concerning the analytical procedures are reported elsewhere (Carena et al., 2017). The results of these determinations are reported in **Table SM1** in the Supplementary Material (hereafter SM). The DOC of our lake water samples, taken near the shore and potentially affected by terrestrial organic matter, was often higher than typical values obtained in the center of the lake, especially in the case of Lago Maggiore (Bertoni et al., 2010). Absorption spectra were taken with an Agilent Technologies Cary 100 double-beam UV-visible spectrophotometer, using 1-cm quartz cuvettes (and 5-cm ones in the case of lake and paddy water). The absorption spectra of HSDZ and SDZ<sup>-</sup> are reported in **Figure SM1**(SM), those of the studied natural water samples in **Figure 1**. The pH of the studied solutions was measured with a Thermo Scientific Orion® model 8115SC Ross™ combination semi-micro pH electrode, connected to a Metrohm model 632 pH meter.

The electron donating capacity (EDC) of the lake and paddy waters, expressed in molar concentration units, was determined employing the recently developed size exclusion

chromatographic (SEC) method which uses a post-column reaction with the stable radical anion of 2,2'-azino-bis(3-ethylbenzothiazoline-6-sulfonate), ABTS<sup>•-</sup> (Chon et al., 2015). Briefly, samples of the waters (2.5 mL) were injected in a Dionex Ultimate 3000 HPLC system (ThermoScientific, Sunnyvale, CA, USA) equipped with a quaternary pump (low-pressure mixing), an autosampler, a thermostated column compartment, a photodiode array UV-vis absorbance detector (PAD) and a variable wavelength UV-vis absorbance detector (VWD). Chromatography was performed on a Toyopearl HW-50S column (8 × 300 mm, 30 μm) (Grace Davison product from BGB, Boeckten, Switzerland), using a 50 mM borate buffer as the eluent at a flow rate of 0.2 mL min<sup>-1</sup>. After the PAD, which recorded the absorbance signal at 254 nm after the exit of the column, the outflow was mixed with the reagent, an ABTS<sup>•-</sup> solution that was delivered at a flow rate of 0.04 mL min<sup>-1</sup> using a Dionex PC 10 system. The mixture then passed a 750 μL knitted reaction coil (Dionex) and the VWD set to record absorbance at 405 nm. Quantification of the EDC was performed by integrating the (negative) peak of decreased ABTS<sup>•-</sup> absorbance, as detailed elsewhere (Chon et al., 2015).

#### ***2.4. Photochemical modelling***

The model assessment of SDZ photodegradation was carried out with the APEX software (Aqueous Photochemistry of Environmentally-occurring Xenobiotics), available for free as Electronic Supplementary Information of Bodrato and Vione (2014). APEX predicts photochemical reaction kinetics from photoreactivity parameters (absorption spectra, direct photolysis quantum yields and second-order reaction rate constants with transient species) and from data of water chemistry and depth (Bodrato and Vione, 2014; Vione, 2014). APEX predictions have been validated by comparison with field data of pollutant phototransformation kinetics in surface freshwaters (see for instance Maddigapu et al., 2011; Marchetti et al., 2013; Bodrato and Vione, 2014).

APEX uses a fair-weather summertime solar spectrum at mid latitude (see **Figure SM1** in the SM) (Frank and Klöpffer, 1988). Sunlight irradiance is not constant in the natural environment due

to fluctuations in meteorological conditions (not included in APEX) and of diurnal and seasonal cycles. To allow easier comparison between model results and environmental conditions, APEX uses as time unit a 24-h summer sunny day (SSD), equivalent to fair-weather 15 July at 45° N latitude, which takes the day-night cycle into account. The absorption of radiation by the photosensitizers (CDOM, nitrate and nitrite) and the target substrate is calculated based on competition for sunlight irradiance in a Lambert-Beer approach (Bodrato and Vione, 2014; Braslavsky, 2007). APEX applies to well-mixed waters and gives average values over the water column, which includes the contributions of the well-illuminated surface layer and of darker water in the lower depths, where irradiance is very low (Loiselle et al., 2008).

In the case of SDZ, literature data were used for the direct photolysis quantum yields and the second-order reaction rate constants with  $\bullet\text{OH}$  and  $^1\text{O}_2$  (see **Table 1**; Boreen et al., 2005). While separate photolysis quantum yields are reported for the two forms HSDZ and  $\text{SDZ}^-$ , no separate  $\bullet\text{OH}$  and  $^1\text{O}_2$  rate constant values are available. In the case of  $^1\text{O}_2$ , this is a minor problem because the reaction plays a negligible role in SDZ phototransformation (*vide infra*). Similar reaction rate constants between SDZ and  $\bullet\text{OH}$  have been measured at presumably acidic pH (Fenton reaction) and at pH around 8 ( $\text{H}_2\text{O}_2$  photolysis), where there is prevalence of HSDZ and  $\text{SDZ}^-$ , respectively (Boreen et al., 2005; Baeza and Knappe, 2011). Moreover, successful modeling of SDZ phototransformation by  $\bullet\text{OH}$  in the  $\text{H}_2\text{O}_2/\text{UV}$  process has been carried out with a single reaction rate constant, in the pH range from 6.5 (comparable values of HSDZ and  $\text{SDZ}^-$ ) to 8.4 (strong prevalence of  $\text{SDZ}^-$ ) (Wols et al., 2014).

As far as the triplet-sensitized transformation is concerned, the reported second-order quenching constants of HSDZ and  $\text{SDZ}^-$  with the triplet state of 4-carboxybenzophenone ( $^3\text{CBBP}^*$ ) (Li et al., 2015) were taken as representative of the corresponding  $^3\text{CDOM}^*$  rate constants. This procedure has been recently shown to be appropriate in the cases of diclofenac, naproxen and clofibric acid (Avetta et al., 2016).

Triplet-sensitized degradation is triggered by reaction between SDZ and  $^3\text{CDOM}^*$  (Boreen et al., 2005), and it is inhibited by DOM antioxidant moieties (Canonica and Launscher, 2008; Wenk and Canonica, 2012; Bahnmüller et al., 2014; Wenk et al., 2015). This effect is not due to a decrease of the rate of the primary reaction, but rather to the back-reduction of partially oxidized SDZ to the parent compound. Such an observation can be summarized by the following equation:

$$k_{\text{SDZ(AO)}} = \psi k_{\text{SDZ}} \quad (1)$$

where  $k_{\text{SDZ(AO)}}$  is the pseudo-first order rate constant of SDZ transformation (either HSDZ or SDZ<sup>-</sup>) triggered by  $^3\text{CDOM}^*$  (or a surrogate of it, e.g.,  $^3\text{CBBP}^*$ ) in the presence of phenolic antioxidants (AO),  $k_{\text{SDZ}}$  is the pseudo-first order rate constant without antioxidants, and  $\psi \leq 1$  is the ratio of the two rate constants. Because the triplet-sensitization process is a bimolecular reaction between SDZ and  $^3\text{CDOM}^*$ , and because  $^3\text{CDOM}^*$  is in steady-state conditions (Canonica et al., 2005; Boreen et al., 2005), one has  $k_{\text{SDZ}} = k_{\text{SDZ},^3\text{CDOM}^*} [^3\text{CDOM}^*]$ , where  $k_{\text{SDZ},^3\text{CDOM}^*}$  is the second-order reaction rate constant between SDZ and  $^3\text{CDOM}^*$ . In the presence of antioxidant molecules, the back-reduction processes decrease the apparent degradation rate of SDZ. To enable this antioxidant effect to be taken into account within APEX, the second-order reaction rate constant for SDZ transformation was modified into an apparent rate constant ( $k_{\text{SDZ},^3\text{CDOM}^*(\text{AO})}$ ) that is lower than the actual one, measured in the absence of antioxidants. One has:

$$k_{\text{SDZ(AO)}} = \psi k_{\text{SDZ}} = \psi k_{\text{SDZ},^3\text{CDOM}^*} [^3\text{CDOM}^*] = k_{\text{SDZ},^3\text{CDOM}^*(\text{AO})} [^3\text{CDOM}^*] \quad (2)$$

from which one gets that  $k_{\text{SDZ},^3\text{CDOM}^*(\text{AO})} = \psi k_{\text{SDZ},^3\text{CDOM}^*}$ . In this way, the antioxidant effect on the degradation kinetics is seen as an apparent decrease of the second-order reaction rate constant at

equal [ $^3\text{CDOM}^*$ ]. This is reasonable because, under conditions that are significant for surface water bodies, dissolved organic compounds including DOM antioxidants are usually unable to quench a significant fraction of the photogenerated triplet states. Therefore, DOM does not affect the steady-state [ $^3\text{CDOM}^*$ ] significantly (Wenk et al., 2013). Finally, the APEX modeling returns also the steady-state [ $^3\text{CDOM}^*$ ] for given water conditions and water depth, referred to a standard sunlight spectrum that corresponds to  $22 \text{ W m}^{-2}$  UV irradiance (Bodrato and Vione, 2014).

### 3. Results and Discussion

#### *3.1. Triplet-sensitized SDZ photodegradation: Effect of phenol as model antioxidant*

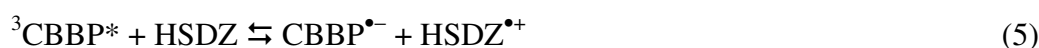
Our first goal was the quantification of the antioxidant effect on the triplet-sensitized degradation of SDZ. The two SDZ forms (acidic HSDZ and basic  $\text{SDZ}^-$ ) are known to react with  $^3\text{CBBP}^*$  to produce oxidation intermediates that may further react to yield transformation products. To assess the possible effect of back reduction on this reaction we chose phenol as model antioxidant, based on the fact that phenol is degraded by direct reaction with  $^3\text{CBBP}^*$  at a lesser extent than other model antioxidants including 4-methylphenol (Canonica and Laubscher, 2008). Because both  $^3\text{CBBP}^*$  quenching and the back-reduction of partially oxidized SDZ are able to inhibit SDZ photodegradation, the use of phenol minimizes the quenching process and should allow the back reduction to be highlighted. The possible consumption of  $^3\text{CBBP}^*$  by phenol was assessed by considering the  $^3\text{CBBP}^*$  decay kinetics ( $k_{3\text{CBBP}^*} = 6 \times 10^5 \text{ s}^{-1}$  in aerated solution; De Laurentiis et al., 2013) and an upper limit for the rate constant of  $^3\text{CBBP}^*$  quenching by phenol ( $k' = 5 \times 10^9 \text{ M}^{-1} \text{ s}^{-1}$ ), which is a typical upper limit for most triplet-sensitized reactions (McNeill and Canonica, 2016).

Considering that HSDZ has  $pK_a \sim 6.5$  (Lin et al., 1997; Sanli et al., 2010) and the carboxylic group of CBBP has  $pK_a \sim 4.5$  (NIST, 2004), the HSDZ experiments were carried out at pH 5.5 to have most SDZ in the protonated form and most CBBP in the deprotonated one. In contrast, the  $SDZ^-$  experiments were carried out at pH 8.5 where CBBP is deprotonated as well (pH was adjusted with a phosphate buffer in both cases). **Figure 2a** reports the time trend of 5  $\mu M$  SDZ in the presence of 40  $\mu M$  CBBP at pH 5.5, with different concentration values of phenol ( $\leq 10 \mu M$  to minimize  $^3CBBP^*$  quenching). The time trend of HSDZ direct photolysis is also reported on the graph, showing that the direct photolysis process was practically negligible. No reliable direct photolysis quantum yield could be inferred from these data. The insert in the figure shows the measured first-order rate constants of HSDZ degradation ( $k_{HSDZ}$ ) as a function of phenol concentration, together with the expected effect of phenol if it only acted as  $^3CBBP^*$  quencher, which appears to be a minor process. The observed experimental trend of  $k_{HSDZ}$  could be fitted well with equation (3). This equation is analogous to the equations derived in previous studies of the inhibitory effect of DOM and model antioxidants on the excited triplet-induced transformation of organic contaminants (Canonica and Laubscher, 2008; Wenk et al., 2011; Wenk and Canonica, 2012).

$$k_{HSDZ} = k_{HSDZ}^o \frac{1}{1 + \frac{[Phenol]}{[Phenol]_{1/2}}} \quad (3)$$

where  $k_{HSDZ}^o$  is the pseudo-first order rate constant in the absence of phenol, and  $[Phenol]_{1/2} = 19.5 \pm 2.5 \mu M$  is the phenol concentration that halves the observed degradation rate constant (hereafter, error bounds represent standard errors). Note that  $\psi = 1/(1 + [Phenol]/[Phenol]_{1/2})$  (see the definition of  $\psi$  in equation 1). The underlying concept of equation (3) is explained in the *Introduction*.

**Figure 2b** reports the time trend of 5  $\mu\text{M}$  SDZ in the presence of 40  $\mu\text{M}$  CBBP at pH 8.5, with different phenol concentrations. The direct photolysis of  $\text{SDZ}^-$ , also reported in the diagram, was slow but its rate constants could be quantified. By applying previously described actinometric methods (Canonica et al., 2008) and using the spectral data of the filtered TQ718 lamp (Leresche et al., 2016), a direct photolysis quantum yield of  $(1.0 \pm 0.1) \times 10^{-3}$  was determined, which is close to that known from literature (see Boreen et al., 2005, and Table 1). The figure insert reports  $k_{\text{SDZ}^-}$  vs. [Phenol], as well as the expected effect of  $^3\text{CBBP}^*$  quenching by phenol itself. A comparison between **Figure 2b** and **Figure 2a** suggests that the inhibitory effect of phenol was more marked in the case of  $\text{SDZ}^-$  compared to HSDZ. The numerical fit of the  $k_{\text{SDZ}^-}$  vs. [Phenol] data with the equivalent of equation (3), obtained by replacing HSDZ with  $\text{SDZ}^-$ , yielded  $[\text{Phenol}]_{1/2} = 0.86 \pm 0.10$   $\mu\text{M}$ . The different effects of phenol at the two investigated pH values might be accounted for by two phenomena: (i) phenol has  $\text{pK}_a \sim 10$  (Martell et al., 1997), and the fraction of phenolate at pH 8.5 is  $10^3$  times higher than at pH 5.5. Phenolate is a stronger reducing agent compared to phenol (Wardman, 1989), thus it can be reasonable that its antioxidant action is more effective. Interestingly, humic substances have been shown to have an increasing antioxidant action (expressed as EDC) with increasing pH (Aeschbacher et al., 2012), which might be accounted for by the occurrence of phenolate anions at the higher pH values; (ii) the radical species derived from the triplet-sensitized oxidation of HSDZ and  $\text{SDZ}^-$  are probably different, but they can undergo an acid-base equilibrium in a similar way as the parent compounds (Tentscher et al., 2013):



However, it is not known whether these acid-base reactions occur on a similar time scale as other transformation/recombination processes relevant for the degradation of SDZ. The very different effects of phenol at pH 5.5 and 8.5 would suggest that the radical species of SDZ do not interconvert quickly.

### **3.2. Photodegradation of SDZ in natural water samples**

SDZ was spiked to the six studied natural water samples to reach an initial concentration of 5  $\mu\text{M}$ , and these systems were then irradiated for up to 4.5 hours. Two blank runs (direct photolysis) were also carried out, at pH 5.5 (HSDZ) and 8.5 ( $\text{SDZ}^-$ ). The pH values of natural water were included in the 7-8 range, thereby ensuring a prevalence of  $\text{SDZ}^-$ . Fully comparable irradiation experiments were carried out with 5  $\mu\text{M}$  TMP, which undergoes triplet-sensitized oxidation with similar rate constant as SDZ, but does not undergo back-reduction upon reaction with antioxidants (Canonica and Laubscher, 2008; Wenk et al., 2015). In the case of TMP, 3 h irradiation was enough to attain complete photodegradation in all the natural waters, except for Lago Maggiore (M). **Figure 3a** reports the initial degradation rates of TMP and SDZ ( $R_{\text{TMP}}$  and  $R_{\text{SDZ}}$ , respectively) observed in the different cases. The lake water samples are shown in order of increasing DOC. Note that S (Santhià) and SG (S. Germano Vercellese) represent paddy-water samples, the DOC values of which were intermediate between those of Candia (C) and Viverone (V). The direct photolysis of TMP and SDZ was practically negligible, except for SDZ at pH 8.5 ( $\text{SDZ}^-$ ). The faster direct photolysis of  $\text{SDZ}^-$  compared to HSDZ is consistent with previous reports (Bian and Zhang, 2016), but the rate of  $\text{SDZ}^-$  direct photolysis was much lower than the photodegradation rate we observed in natural water samples. Therefore, the photodegradation of SDZ in our natural water samples, under our irradiation conditions, should mainly take place by indirect photochemistry. The photodegradation of TMP was particularly effective in paddy water. In the case of lake water the



TMP transformation rate increased with increasing DOC, as can be expected for a process that involves  $^3\text{CDOM}^*$  but is not affected by back-reduction (Canonica and Laubscher, 2008; Bodhipaksha et al., 2015). Compared to TMP, the phototransformation kinetics of SDZ showed a much less marked dependence on the DOC of either lake- or paddy-water. Similar results have already been reported in the case of SDZ irradiated in river water (Bahnmüller et al., 2014).

Paddy water had no peculiarly high DOC when compared to the investigated lake water, but it had higher absorbance (see **Figure 1**). Interestingly, the plot of  $R_{\text{TMP}}$  vs. the 300-nm absorbance of natural water ( $A_1(300\text{nm})$ ), see **Figure 3b**) yielded a reasonably straight line. It is suggested that the kinetics of TMP photodegradation with respect to the amount of absorbed radiation were very similar in all the studied natural water samples. In contrast,  $R_{\text{SDZ}}$  reached a plateau already at relatively low values of  $A_1(300\text{nm})$ . The rationale for taking the water absorbance into account is that CDOM is both the  $^3\text{CDOM}^*$  source and the main light-absorbing species in natural waters between 300 and 500 nm (Loiselle et al., 2008). The present finding concerning  $R_{\text{TMP}}$  vs.  $A_1(300\text{nm})$  is consistent with a previous report that the quantum yield of  $^3\text{CDOM}^*$  photogeneration was comparable in paddy- and lake-water (Carena et al., 2017). TMP at the used initial concentration (5  $\mu\text{M}$ ) would carry out a minor quenching of  $^3\text{CDOM}^*$  (Canonica et al., 2001). This issue allows for the use of the relationship  $R_{\text{TMP}} = k_{\text{TMP},^3\text{CDOM}^*}[\text{TMP}][^3\text{CDOM}^*]$  to derive a  $[^3\text{CDOM}^*]$  value that would be valid in the absence of TMP as well. Thus, by assuming  $k_{\text{TMP},^3\text{CDOM}^*} = 3 \times 10^9 \text{ M}^{-1} \text{ s}^{-1}$  (Al Housari et al., 2010), the  $[^3\text{CDOM}^*]$  values that are reported in the right Y-axis of **Figure 3b** were obtained as  $[^3\text{CDOM}^*] = R_{\text{TMP}} / ([\text{TMP}] \times (3 \times 10^9 \text{ M}^{-1} \text{ s}^{-1}))$ .

Differently from TMP, SDZ could undergo different transformation processes including the direct photolysis and the reactions with  $\bullet\text{OH}$  and  $^3\text{CDOM}^*$ . However, the 0.15 M nitrate solution used to filter lamp radiation would largely reduce the photon flux absorbed by both SDZ and nitrate in the samples, thereby minimizing both direct photolysis and  $\bullet\text{OH}$  reactions. As a consequence, the

primary reaction between SDZ and  $^3\text{CDOM}^*$  is potentially important in SDZ degradation, but the overall process would be inhibited by the back reactions between oxidized SDZ and DOM antioxidants (Canonica and Laubscher, 2008; Wenk et al., 2015).

It is possible to assess the importance of the SDZ back reactions in the irradiated samples by comparing the ratio of the degradation rates of TMP and SDZ ( $R_{\text{TMP}}(R_{\text{SDZ}})^{-1}$ ) with the electron-donating capacity of the samples (EDC, units of  $\mu\text{mol e}^- \text{L}^{-1}$ , see **Table SM1**). The EDC parameter measures the molar concentration of DOM antioxidants. Considering that SDZ undergoes back-reactions with DOM antioxidants while TMP does not (Wenk et al., 2015), the higher is the EDC, the higher is expected to be the  $R_{\text{TMP}}(R_{\text{SDZ}})^{-1}$  ratio if TMP and SDZ mostly react with  $^3\text{CDOM}^*$ .

**Figure 3c** reports the correlation plot between  $R_{\text{TMP}}(R_{\text{SDZ}})^{-1}$  and the measured EDC, which suggests a very good linear trend. Interestingly, the paddy fields showed higher values of EDC per unit DOC compared to lake water. The reason is possibly linked to the fact that the biological processing of DOM in paddy water is so high that the organic matter is renewed very quickly and has little time to undergo photochemical oxidation (Carena et al., 2017).

### 3.3. Modeling of SDZ phototransformation

#### 3.3.1. Model validation

As already mentioned, to model the effect of DOM antioxidant moieties on the triplet-sensitized degradation of SDZ (either HSDZ or  $\text{SDZ}^-$ ), it was assumed a decrease of the relevant second-order reaction rate constants. We used  $k_{\text{SDZ},^3\text{CDOM}^*(\text{AO})} = \psi k_{\text{SDZ},^3\text{CDOM}^*}$ , with  $\psi = (1 + [\text{Phenol}]([\text{Phenol}]_{1/2})^{-1})^{-1}$  as per equation (3). The main difficulty with this approach is that the natural DOM contains phenolic compounds, among other functionalities, but it is not only made up of phenols. The phenolic content of specific DOM samples is known (Ritchie and Perdue,

2003), but one should make the additional hypothesis that natural DOM phenols have the same or similar antioxidant effect as the phenol molecule. Fortunately, the antioxidant effect of phenol has been compared with that of Suwannee River Fulvic Acids (SRFA) and of Pony Lake Fulvic Acids (PLFA) in the case of the triplet-sensitized transformation of *N,N*-dimethyl-4-cyanoaniline (Leresche et al., 2016). The substrate degradation rate was halved in the presence of  $[\text{Phenol}]_{1/2} = 3.7 \mu\text{mol L}^{-1}$ , of  $[\text{DOM}]_{1/2} = 3.2 \text{ mgC L}^{-1}$  (PLFA), or of  $[\text{DOM}]_{1/2} = 1.5 \text{ mgC L}^{-1}$  (SRFA). These concentration values allow for the determination of the phenol antioxidant equivalents of PLFA and SRFA. Therefore, the value of  $[\text{Phenol}]_{1/2} \sim 19 \mu\text{mol L}^{-1}$  we obtained for HSDZ would correspond to  $[\text{DOM}]_{1/2} \sim 17 \text{ mgC L}^{-1}$  PLFA, or to  $\sim 8 \text{ mgC L}^{-1}$  SRFA. Similarly, the value of  $[\text{Phenol}]_{1/2} \sim 0.9 \mu\text{mol L}^{-1}$  we obtained for SDZ<sup>-</sup> would correspond to  $[\text{DOM}]_{1/2} \sim 0.7 \text{ mgC L}^{-1}$  PLFA, or to  $\sim 0.3 \text{ mgC L}^{-1}$  SRFA. We used these  $[\text{DOM}]_{1/2}$  values for the modeling of HSDZ and SDZ<sup>-</sup> phototransformation, assuming  $\psi = (1 + \text{DOC}([\text{DOM}]_{1/2})^{-1})^{-1}$ .

It should be noted here that humic substances such as PLFA and SRFA are not the only DOM components with phenolic moieties or antioxidant behavior. Other examples include for instance the tyrosine groups of peptides (Coble, 1996), thus the degree by which PLFA or SRFA are representative of the antioxidant DOM moieties has to be assessed. Anyway, in addition to being the only substances with available  $[\text{DOM}]_{1/2}$  data, these humic compounds make a reasonable choice because SRFA is routinely used in the quality control of EDC measurements (Chon et al., 2015). Moreover, the fluorescence spectra of the paddy water samples used in our irradiation experiments have shown a strong prevalence of humic substances compared to proteins (Carena et al., 2017).

The APEX software uses a standard sunlight spectrum for modeling, under which conditions it is well known that SDZ undergoes significant direct photolysis (Bahnmüller et al., 2014). In contrast, we chose the irradiation set-up to highlight only the triplet-sensitized phototransformation of SDZ. Therefore, the validation of model predictions with the experimental data was carried out

by considering the predicted SDZ phototransformation kinetics accounted for by  $^3\text{CDOM}^*$  alone. To avoid problems linked with the different irradiation sources, we used the steady-state  $[\text{}^3\text{CDOM}^*]$  to achieve a normalization between experimental data and model predictions. The experimental  $[\text{}^3\text{CDOM}^*]$  values are those obtained from the TMP phototransformation kinetics, and they are reported in **Figure 3b**. The corresponding predicted values of  $[\text{}^3\text{CDOM}^*]$  were obtained by adjusting the model parameters and by varying the input DOC, so that the modeled  $[\text{}^3\text{CDOM}^*]$  values matched the experimental ones. Note that, for short optical path lengths (in the model it was used a water depth  $d = 1$  cm that is close to the optical path length of the experiments) there is a direct proportionality between  $[\text{}^3\text{CDOM}^*]$  and DOC. The match was carried out so that the model predicted  $[\text{}^3\text{CDOM}^*] = 5 \times 10^{-13}$  M for  $\text{DOC} = 10 \text{ mgC L}^{-1}$ . This value is not far from the DOC values of the paddy water samples that yielded the highest experimental  $[\text{}^3\text{CDOM}^*]$ . Finally, because APEX returns first-order rate constants and not initial transformation rates, the predicted rate constants were transformed into  $[\text{s}^{-1}]$  units and multiplied by  $[\text{SDZ}]_0 = 5 \text{ }\mu\text{M}$  to get the predicted initial rates  $R_{\text{SDZ}}$ .

The experimental  $R_{\text{SDZ}}$  data reported in **Figure 4a/b** are the same as those of **Figure 3b**, including the same meaning for open and solid symbols in repeated experiments, but they are plotted as a function of the experimental  $[\text{}^3\text{CDOM}^*]$ . Because two TMP degradation replicas were carried out for each condition, the used  $[\text{}^3\text{CDOM}^*]$  is the average of the values obtained in both sets of experiments. In **Figure 4a**, the experimental data are compared with the model predictions in the PLFA-like scenario for HSDZ ( $[\text{DOM}]_{1/2} = 17 \text{ mgC L}^{-1}$ ), for  $\text{SDZ}^-$  ( $[\text{DOM}]_{1/2} = 0.7 \text{ mgC L}^{-1}$ ), and for a mixture containing 30% HSDZ + 70%  $\text{SDZ}^-$ . Such a mixture would be observed at  $\text{pH} \sim 7$ . In the case of the mixture, one finds a reasonable agreement between model predictions and experimental data. In **Figure 4b**, the same comparison is made in the SRFA-like scenario ( $[\text{DOM}]_{1/2} \sim 8 \text{ mgC L}^{-1}$  for HSDZ and  $0.3 \text{ mgC L}^{-1}$  for  $\text{SDZ}^-$ ), where the impact of back reduction is considerably higher than for PLFA. The mixture of 30% HSDZ + 70%  $\text{SDZ}^-$  did not match the

experimental data as well as in the previous case; a better match with the experiments would be obtained with 50% HSDZ + 50% SDZ<sup>-</sup>, but that would imply pH 6.5 that is not really compatible with the pH values of the studied water samples (see SM). In summary, the PLFA-like scenario gave a somewhat better match with the experimental data than the SRFA-like scenario.

### 3.3.2. Modeling of SDZ photodegradation under conditions representative of natural waters

Thus far, only the reaction between SDZ and <sup>3</sup>CDOM\* was modeled to allow for a comparison with the irradiation experiments. By taking into account all the main phototransformation processes (see **Table 1** for the relevant kinetic parameters), one obtains the results reported in **Figure 5**. These results should give insight into the actual behavior of SDZ in natural waters. **Figure 5a** reports the modeled fractions of SDZ transformation accounted for by the different photoreactions as a function of pH, for  $d = 5$  m and DOC = 3 mgC L<sup>-1</sup>. When pH increases one has an increasing percentage of SDZ<sup>-</sup> with respect to HSDZ ( $pK_a = 6.5$ ). Moreover, HSDZ and SDZ<sup>-</sup> have similar phototransformation rate constants for DOC = 3 mgC L<sup>-1</sup> (*vide infra*). The plot shows that the <sup>3</sup>CDOM\* process would prevail in the case of HSDZ, and that it would be gradually replaced by the direct photolysis as the SDZ<sup>-</sup> fraction gets higher. In either case, the <sup>•</sup>OH reaction would only play a secondary role. Note that these conclusions are obtained for the PLFA-like scenario, but very similar results apply to the SRFA-like case as well.

**Figure 5b** reports the predicted half-lives of HSDZ and SDZ<sup>-</sup> in the PLFA-like and SRFA-like scenarios, as a function of the DOC for  $d = 5$  m. The predicted half-lives increase with increasing DOC and, depending on the SDZ form and the modeled scenario, they vary from some days to several weeks. Similar transformation kinetics are predicted for HSDZ and SDZ<sup>-</sup> at DOC = 2-3 mgC L<sup>-1</sup>, with very few differences between the SRFA-like and the PLFA-like scenarios. At lower DOC one expects the phototransformation of SDZ<sup>-</sup> to be slightly faster than that of HSDZ, while the reverse happens at higher DOC. In particular, for DOC = 10 mgC L<sup>-1</sup> the phototransformation

of HSDZ would be considerably faster than that of  $\text{SDZ}^-$ . In these DOC conditions, the predicted half-lives are expected to significantly increase (and the relevant rate constants to correspondingly decrease) with increasing pH.

The steady-state [ $^3\text{CDOM}^*$ ] increases with increasing DOC, while other processes such as direct photolysis and  $\bullet\text{OH}$  reactions are inhibited in high-DOC waters (Vione et al., 2014). Increasing DOC would on the one side enhance the primary reaction of SDZ with  $^3\text{CDOM}^*$  but, on the other hand, it would also enhance back reduction. It is interesting to see the expected impact of these two contrasting effects on the importance of  $^3\text{CDOM}^*$  in the photodegradation of HSDZ and  $\text{SDZ}^-$ , as the DOC increases. The plots shown in **Figures 5c-f** report, as a function of the DOC and for  $d = 5$  m, the modeled fractions of HSDZ or  $\text{SDZ}^-$  that undergo transformation *via* the different photoreaction pathways, in the SRFA-like and PLFA-like scenarios. The  $\bullet\text{OH}$  process undergoes the highest inhibition with increasing DOC, due to the scavenging of  $\bullet\text{OH}$  by DOM (Vione et al., 2014). The direct photolysis is also inhibited with increasing DOC, due to competition between HSDZ/ $\text{SDZ}^-$  and CDOM for sunlight irradiance. However, the direct photolysis undergoes lesser inhibition compared to the  $\bullet\text{OH}$  reaction, which accounts for the trend with a maximum of the direct photolysis fraction as a function of the DOC. Very interestingly, the relative importance of the  $^3\text{CDOM}^*$  process is predicted to increase with the DOC in all the investigated scenarios, including the SRFA-like case with  $\text{SDZ}^-$ . This is the scenario where the impact of back reduction is expected to be the highest.

To explain the above finding, one should consider that the kinetics of all the processes are slowed down when the DOC is high. The  $\bullet\text{OH}$  reaction is inhibited by DOM scavenging, while CDOM inhibits the direct photolysis by competition for irradiance. The combination of CDOM absorption saturation and back reduction slows down the degradation induced by  $^3\text{CDOM}^*$ , but to a lesser extent compared to the other two pathways. As a result, even in the presence of the

antioxidant-induced reduction process, the relative importance of triplet-sensitized degradation is predicted to increase with increasing DOC.

## 4. Conclusions

- Phenolic antioxidants are able to inhibit the triplet-sensitized degradation of SDZ. The inhibition effect can be assessed in the laboratory by using model phenolic compounds (phenol in the present case), provided that they do not significantly quench the photogenerated triplet states. The use of the equivalent anti-oxidant behavior of SRFA or PLFA was here shown to be appropriate to extrapolate the laboratory results to the behavior of DOM in natural water samples. The PLFA-like case allowed for a better agreement with the experimental data.
- The inhibition effect of phenol was more marked with the anionic form ( $\text{SDZ}^-$ ) than with the neutral one (HSDZ). The extent of the inhibition was directly proportional to the electron-donating capacity of the water sample. Therefore, at least for short optical path lengths that are typical of laboratory irradiation set-ups, the kinetics of SDZ phototransformation was poorly dependent on the amount of (C)DOM in the studied water samples.
- In sunlit surface waters, direct photolysis and  $\bullet\text{OH}$  reaction are expected to account for the majority of the photodegradation of both HSDZ and  $\text{SDZ}^-$  if the DOC is low ( $< 1 \text{ mgC L}^{-1}$ ). With higher DOC ( $> 3\text{-}4 \text{ mgC L}^{-1}$ ) and despite the back-reduction processes, the  $^3\text{CDOM}^*$  reactions would account for the majority of HSDZ phototransformation. In the case of  $\text{SDZ}^-$  at high DOC, the direct photolysis would be the main phototransformation process.
- Interestingly, although the  $^3\text{CDOM}^*$  reactions are secondary processes for  $\text{SDZ}^-$  in natural-water settings, their relative importance is expected to increase with increasing DOC despite the considerable back-reduction phenomenon. Back-reduction is observed with several compounds, and particularly with those having amine or sulfonamide groups (Canonica and Laubscher,

2008; Davis et al., 2017). Our findings suggest that, for many xenobiotics undergoing back reduction, the process inhibition by DOM would not prevent triplet sensitization from gaining importance with increasing DOC. In several cases, the  $^3\text{CDOM}^*$  reaction could still become the main photoprocesses in DOM-rich (i.e., high-DOC) waters.

- An increase in water pH shifts the prevailing SDZ form from HSDZ to  $\text{SDZ}^-$ , and it would enhance the direct photolysis at the expense of triplet sensitization. When taking into account the possible variations of surface-water conditions, SDZ is expected to be fairly photolabile under summertime sunlight: the photochemical half-lives would range from a few days to a couple of months, which in many cases would successfully compete with the biodegradation kinetics.
- To extend this study to other compounds, it is necessary to know or measure their reaction rate constants with a reactive triplet state (e.g.,  $^3\text{CBBP}^*$ ), and to assess the values of  $[\text{Phenol}]_{1/2}$  or  $[\text{DOM}]_{1/2}$  under conditions of triplet sensitization and back-reduction.

### *Acknowledgements*

The authors are very grateful to Ursula Schönenberger for technical assistance in Dübendorf, as well as to Elisabeth Salhi for performing the EDC analysis of the natural water samples. DV and SC acknowledge the Swiss National Science Foundation (grant number IZK0Z2\_173662 / 1) that supported a one-month stay of DV in Dübendorf. DV and MM also acknowledge support from MIUR-PNRA and from Compagnia di San Paolo (project CSTO168282 ABATEPHARM).



## References

- Adamek, E., Baran, W., Sobczak, A., 2016. Assessment of the biodegradability of selected sulfa drugs in two polluted rivers in Poland: Effects of seasonal variations, accidental contamination, turbidity and salinity. *J. Hazard. Mater.* 313, 147-158.
- Aeschbacher, M., Graf, C., Schwarzenbach, R.P., Sander, M., 2012. Antioxidant properties of humic substances. *Environ. Sci. Technol.* 46, 4916-4925.
- Al Housari, F., Vione, D., Chiron, S., Barbati, S., 2010. Reactive photoinduced species in estuarine waters. Characterization of hydroxyl radical, singlet oxygen and dissolved organic matter triplet state in natural oxidation processes. *Photochem. Photobiol. Sci.* 9, 78-86.
- Avetta, P., Fabbri, D., Minella, M., Brigante, M., Maurino, V., Minero, C., Pazzi, M., Vione, D., 2016. Assessing the phototransformation of diclofenac, clofibric acid and naproxen in surface waters: Model predictions and comparison with field data. *Water Res.* 105, 383-394.
- Baeza, C., Knappe, D. R. U., 2011. Transformation kinetics of biochemically active compounds in low-pressure UV Photolysis and UV/H<sub>2</sub>O<sub>2</sub> advanced oxidation processes. *Water Res.* 45, 4531-4543.
- Bahn Müller, S., von Gunten, U., Canonica, S., 2014. Sunlight-induced transformation of sulfadiazine and sulfamethoxazole in surface waters and wastewater effluents. *Wat. Res.* 57, 183-192.
- Batista, A. P. S., Cottrell, B. A., Nogueira, R. F. P., 2014. Photochemical transformation of antibiotics by excitation of Fe(III)-complexes in aqueous medium. *J. Photochem. Photobiol. A: Chem.* 274, 50-56.
- Bertoni, R., Callieri, C., Corno, G., Rasconi, S., Caravati, E., Contesini, M., 2010. Long-term trends of epilimnetic and hypolimnetic bacteria and organic carbon in a deep holo-oligomictic lake. *Hydrobiologia* 644, 279-287.

- Bian, X. S., Zhang, J. B., 2016. Photodegradation of sulfadiazine in aqueous solution and the affecting factors. *J. Chem.*, art. n. 8358960.
- Bianco, A., Fabbri, D., Minella, M., Brigante, M., Mailhot, G., Maurino, V., Minero, C., Vione, D., 2015. New insights into the environmental photochemistry of 5-chloro-2-(2,4-dichlorophenoxy)phenol (triclosan): Reconsidering the importance of indirect photoreactions. *Water Res.* 72, 271-280.
- Bodhipaksha, L. C., Sharpless, C. M., Chin, Y. P., Sander, M., Langston, W. K., MacKay, A. A., 2015. Triplet photochemistry of effluent and natural organic matter in whole water and isolates from effluent-receiving rivers. *Environ. Sci. Technol.* 49, 3453-3463.
- Bodrato, M., Vione, D., 2014. APEX (Aqueous Photochemistry of Environmentally occurring Xenobiotics): A free software tool to predict the kinetics of photochemical processes in surface waters. *Environ. Sci.: Processes Impacts* 16, 732-740.
- Boreen, A. L., Arnold, W. A., McNeill, K., 2003. Photodegradation of pharmaceuticals in the aquatic environment: A review. *Aquat. Sci.* 65, 320-341.
- Boreen, A. L., Arnold, W. A., McNeill, K., 2005. Triplet-sensitized photodegradation of sulfa drugs containing six-membered heterocyclic groups: Identification of an SO<sub>2</sub> extrusion photoproduct. *Environ. Sci. Technol.* 39, 3630-3638.
- Braslavsky, S.E., 2007. Glossary of terms used in photochemistry, 3<sup>rd</sup> edition. *Pure Appl. Chem.* 79, 293-465.
- Canonica, S., Freiburghaus, M., 2001. Electron-rich phenols for probing the photochemical reactivity of freshwaters. *Environ. Sci. Technol.* 35, 690-695.
- Canonica, S., Meunier, L., von Gunten, U., 2008. Phototransformation of selected pharmaceuticals during UV treatment of drinking water. *Water Res.* 42, 121-128.
- Canonica, S., Laubscher, H. U., 2008. Inhibitory effect of dissolved organic matter on triplet-induced oxidation of aquatic contaminants. *Photochem. Photobiol. Sci.* 7, 547-551.

- Carena, L., Minella, M., Barsotti, F., Brigante, M., Milan, M., Ferrero, A., Berto, S., Minero, C., Vione, D., 2017. Phototransformation of the herbicide propanil in paddy field water. *Environ. Sci. Technol.* 51, 2695-2704.
- Chen, Y. M., Leung, K. S. Y., Wong, J. W. C., Selvam, A., 2013. Preliminary occurrence studies of antibiotic residues in Hong Kong and Pearl River delta. *Environ. Monit. Assess.* 185, 745-754.
- Chon, K., Salhi, E., von Gunten, U., 2015. Combination of UV absorbance and electron donating capacity to assess degradation of micropollutants and formation of bromate during ozonation of wastewater effluents. *Water Res.* 81, 388-397.
- Coble, P. G., 1996. Characterization of marine and terrestrial DOM in seawater using excitation-emission spectroscopy. *Mar. Chem.* 51, 325-346.
- Cory, R. M., Cotner, J. B., McNeill, K., 2009. Quantifying interactions between singlet oxygen and aquatic fulvic acids. *Environ. Sci. Technol.* 43, 718-723.
- Davis, C. A., Erickson, P. R., McNeill, K., Janssen, E. M. L., 2017. Environmental photochemistry of fenamate NSAIDs and their radical intermediates. *Environmental Sci.: Processes Impacts* 19, 656-665.
- De Laurentiis, E., Minella, M., Maurino, V., Minero, C., Brigante, M., Mailhot, G., Vione, D., 2012. Photochemical production of organic matter triplet states in water samples from mountain lakes, located below or above the treeline. *Chemosphere* 88, 1208-1213.
- De Laurentiis, E., Socorro, J., Vione, D., Quivet, E., Brigante, M., Mailhot, G., Wortham, H., Gligorovski, S., 2013. Phototransformation of 4-phenoxyphenol sensitised by 4-carboxybenzophenone: Evidence of new photochemical pathways in the bulk aqueous phase and on the surface of aerosol deliquescent particles. *Atmos. Environ.* 81, 569-578.
- Diaz, M., Luiz, M., Bertolotti, S., Miskoski, S., Garcia, N. A., 2004. Scavenging of photogenerated singlet molecular oxygen and superoxide radical anion by sulpha drugs - Kinetics and mechanism. *Can. J. Chem.-Rev. Can. Chim.* 82, 1752-1759.

- Dulin, D., Mill, T., 1982. Development and evaluation of sunlight actinometers. *Environ. Sci. Technol.* 16, 815-820.
- Frank, R., Klöpffer, W., 1988. Spectral solar photo irradiance in Central Europe and the adjacent north Sea, *Chemosphere* 17, 985-994.
- Gao, L. H., Shi, Y. L., Li, W. H., Niu, H. Y., Liu, J. M., Cai, Y. Q., 2012. Occurrence of antibiotics in eight sewage treatment plants in Beijing, China. *Chemosphere* 86, 665-671.
- Giang, C. N. D., Sebesvari, Z., Renaud, F., Rosendahl, I., Minh, Q. H., Amelung, W., 2015. Occurrence and dissipation of the antibiotics sulfamethoxazole, sulfadiazine, trimethoprim, and enrofloxacin in the Mekong delta, Vietnam. *Plos One* 10, art. n. e0131855.
- Huang, X. F., Feng, Y., Hu, C., Xiao, X. Y., Yu, D. L., Zou, X. M., 2016. Mechanistic model for interpreting the toxic effects of sulfonamides on nitrification. *J. Hazard. Mater.* 305, 123-129.
- Leresche, F., von Gunten, U., Canonica, S., 2016. Probing the photosensitizing and inhibitory effects of dissolved organic matter by using N,N-dimethyl-4-cyanoaniline (DMABN). *Environ. Sci. Technol.* 50, 10997-11007.
- Li, Y. J., Wei, X. X., Chen, J. W., Xie, H. B., Zhang, Y. N., 2015. Photodegradation mechanism of sulfonamides with excited triplet state dissolved organic matter: A case of sulfadiazine with 4-carboxybenzophenone as a proxy. *J. Hazard. Mater.* 290, 9-15.
- Li, Y. X., Liu, B., Zhang, X. L., Wang, J., Gao, S. Y., 2016a. The distribution of veterinary antibiotics in the river system in a livestock-producing region and interactions between different phases. *Environ. Sci. Pollut. Res.* 23, 16542-16551.
- Li, Y., Li, Q., Zhou, K., Sun, X. L., Zhao, L. R., Zhang, Y. B., 2016b. Occurrence and distribution of the environmental pollutant antibiotics in Gaoqiao mangrove area, China. *Chemosphere* 147, 25-35.
- Li, B., Zhang, T., 2011. Mass flows and removal of antibiotics in two municipal wastewater treatment plants. *Chemosphere* 83, 1284-1289.

- Lin, C. E., Lin, W. C., Chen, Y. C., Wang, S. W., 1997. Migration behavior and selectivity of sulfonamides in capillary electrophoresis. *J. Chromatogr. A* 792, 37-47.
- Loiselle, S. A., Azza, N., Cozar, A., Bracchini, L., Tognazzi, A., Dattilo, A., Rossi, C., 2008. Variability in factors causing light attenuation in Lake Victoria. *Freshwater Biol.* 53, 535-545.
- Mack, J., Bolton, J.R., 1999. Photochemistry of nitrite and nitrate in aqueous solution: a review. *J. Photochem. Photobiol. A: Chem.* 128, 1-13.
- Maddigapu, P.R., Minella, M., Vione, D., Maurino, V., Minero, C., 2011. Modeling phototransformation reactions in surface water bodies: 2,4-Dichloro-6-nitrophenol as a case study. *Environ. Sci. Technol.* 45, 209-214.
- Madigan, M., Martinko, J., Stahl, D., Clark, D., 2012. *Brock Biology of Microorganisms* (13<sup>th</sup> ed.), Pearson Education, 797 pp.
- Marchetti, G., Minella, M., Maurino, V., Minero, C., Vione, D., 2013. Photochemical transformation of atrazine and formation of photointermediates under conditions relevant to sunlit surface waters: Laboratory measures and modelling. *Water Res.* 47, 6211-6222.
- McNeill, K., Canonica, S., 2016. Triplet state dissolved organic matter in aquatic photochemistry: reaction mechanisms, substrate scope, and photophysical properties. *Environ. Sci. Processes Impacts* 18, 1381-1399.
- Minella, M., Leoni, B., Salmaso, N., Savoye, L., Sommaruga, R., Vione, D., 2016. Long-term trends of chemical and modelled photochemical parameters in four Alpine lakes. *Sci. Total Environ.* 541, 247-256.
- NIH, 2017. <https://aidsinfo.nih.gov/drugs/448/sulfadiazine/0/patient>, last accessed August 2017.
- NIST, 2004. Critically Selected Stability Constants of Metal Complexes Database. Standard Reference Data Program, Vol. 46, National Institute of Standards and Technology, U.S. Department of Commerce.

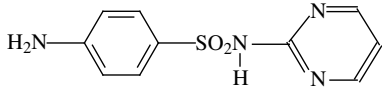
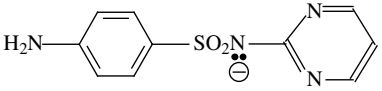
- Pan, S. H., Yan, N., Liu, X. Y., Wang, W. B., Zhang, Y. M., Liu, R., Rittmann, B. E., 2014. How UV photolysis accelerates the biodegradation and mineralization of sulfadiazine (SD). *Biodegradation* 25, 911-921.
- Ritchie, J. D., Perdue, E. M., 2003. Proton-binding study of standard and reference fulvic acids, humic acids, and natural organic matter. *Geochim. Cosmochim. Acta* 67, 85-96.
- Sakai, N., Yusof, R. M., Sapar, M., Yoneda, M., Mohd, M. A., 2016. Spatial analysis and source profiling of beta-agonists and sulfonamides in Langat River basin, Malaysia. *Sci. Total Environ.* 548, 43-50.
- Sanli, N., Sanli, S., Ozkan, G., Denizli, A., 2010. Determination of pK(a) values of some sulfonamides by LC and LC-PDA methods in acetonitrile-water binary mixtures. *J. Brazil. Chem. Soc.* 21, 1952-1960.
- Sun, M., Chang, Z. Q., Van den Brink, P. J., Li, J., Zhao, F. Z., Rico, A., 2016. Environmental and human health risks of antimicrobials used in *Fenneropenaeus chinensis* aquaculture production in China. *Environ. Sci. Pollut. Res.* 23, 15689-15702.
- Tentscher, P.R., Eustis, S.N., McNeill, K., Arey, J.S., 2013. Aqueous oxidation of sulfonamide antibiotics: Aromatic nucleophilic substitution of an aniline radical cation. *Chemistry Eur. J.* 19, 11216-11223.
- Vione, D., 2014. A test of the potentialities of the APEX software (Aqueous Photochemistry of Environmentally-occurring Xenobiotics). Modelling the photochemical persistence of the herbicide cycloxydim in surface waters, based on literature kinetics data. *Chemosphere* 99, 272-275.
- Vione, D., Minella, M., Maurino, V., Minero, C., 2014. Indirect photochemistry in sunlit surface waters: Photoinduced production of reactive transient species. *Chemistry Eur. J.* 20, 10590-10606.
- Vosough, M., Rashvand, M., Esfahani, H. M., Kargosha, K., Salemi, A., 2015. Direct analysis of six antibiotics in wastewater samples using rapid high-performance liquid chromatography

- coupled with diode array detector: A chemometric study towards green analytical chemistry. *Talanta* 135, 7-17.
- Vree, T. B., Schoondermarkvandeven, E., Verweyvanwissen, C. P. W. G. M., Baars, A. M., Swolfs, A., Vangalen, P. M., Amadjaisgroenen, H. Isolation, identification and determination of sulfadiazine and its hydroxy metabolite and conjugates from man and Rhesus-monkey by high-performance liquid chromatography. *J. Chromatogr. B.* 670, 111-123.
- Wardman, P., 1989. Reduction potentials of one-electron couples involving free radicals in aqueous solution. *J. Phys. Chem. Ref. Data* 18, 1637-1755.
- Wenk, J., von Gunten, U., Canonica, S., 2011. Effect of dissolved organic matter on the transformation of contaminants induced by excited triplet states and the hydroxyl radical. *Environ. Sci. Technol.* 45, 1334-1340.
- Wenk, J., Canonica, S., 2012. Phenolic antioxidants inhibit the triplet-induced transformation of anilines and sulfonamide antibiotics in aqueous solution. *Environ. Sci. Technol.* 46, 5455-5462.
- Wenk, J., Eustis, S. N., McNeill, K., Canonica, S., 2013. Quenching of excited triplet states by dissolved natural organic matter. *Environ. Sci. Technol.* 27, 12802-12810.
- Wenk, J., Aeschbacher, M., Sander, M., von Gunten, U., Canonica, S., 2015. Photosensitizing and inhibitory effects of ozonated dissolved organic matter on triplet-induced contaminant transformation. *Environ. Sci. Technol.* 49, 8541-8549.
- WHO, 2017. WHO Model List of Essential Medicines (20th edition, April 2017), 58 pp. [http://www.who.int/medicines/publications/essentialmedicines/20th\\_EML2017\\_FINAL\\_ amendedAug2017.pdf?ua=1](http://www.who.int/medicines/publications/essentialmedicines/20th_EML2017_FINAL_ amendedAug2017.pdf?ua=1), last accessed August 2017.
- Wols, B. A., Harmsen, D. J. H., Beerendonk, E. F., Hofman-Caris, C. H. M., 2014. Predicting pharmaceutical degradation by UV (LP)/H<sub>2</sub>O<sub>2</sub> processes: A kinetic model. *Chem. Eng. J.* 2014, 255, 334-343.

- Yuan, Q. B., Guo, M. T., Yang, J., 2014. Monitoring and assessing the impact of wastewater treatment on release of both antibiotic-resistant bacteria and their typical genes in a Chinese municipal wastewater treatment plant. *Environ. Sci. Processes Impacts* 16, 1930-1937.
- Zhang, J. W., Ma, L., 2013. Photodegradation mechanism of sulfadiazine catalyzed by Fe(III), oxalate and algae under UV irradiation. *Environ. Technol.* 34, 1617-1623. DOI: <http://dx.doi.org/10.1080/09593330.2013.765915>.



**Table 1.** Photoreactivity parameters of the acidic/neutral and basic/anionic forms of SDZ (HSDZ and  $\text{SDZ}^-$ , respectively) (Boreen et al., 2005; Li et al., 2015). Note that  $^3\text{CBBP}^*$  is the excited triplet state of 4-carboxybenzophenone, used as CDOM proxy. The reaction rate constant  $k_{\text{SDZ},^3\text{CBBP}^*}$  was set equal to the second-order rate constant for  $^3\text{CBBP}^*$  quenching by SDZ, available from the literature.

	<b>HSDZ</b>	<b><math>\text{SDZ}^-</math></b>
		
$\Phi_{\text{SDZ}}$ , unitless	$(0.4 \pm 0.2) \times 10^{-3}$	$(1.2 \pm 0.2) \times 10^{-3}$
$k_{\text{SDZ}, \cdot\text{OH}}$ , $\text{M}^{-1} \text{s}^{-1}$	$(3.7 \pm 0.5) \times 10^9$	
$k_{\text{SDZ}, ^1\text{O}_2}$ , $\text{M}^{-1} \text{s}^{-1}$	$8.9 \times 10^6$	
$k_{\text{SDZ}, ^3\text{CBBP}^*}$ , $\text{M}^{-1} \text{s}^{-1}$	$4.9 \times 10^9$	$2.9 \times 10^9$

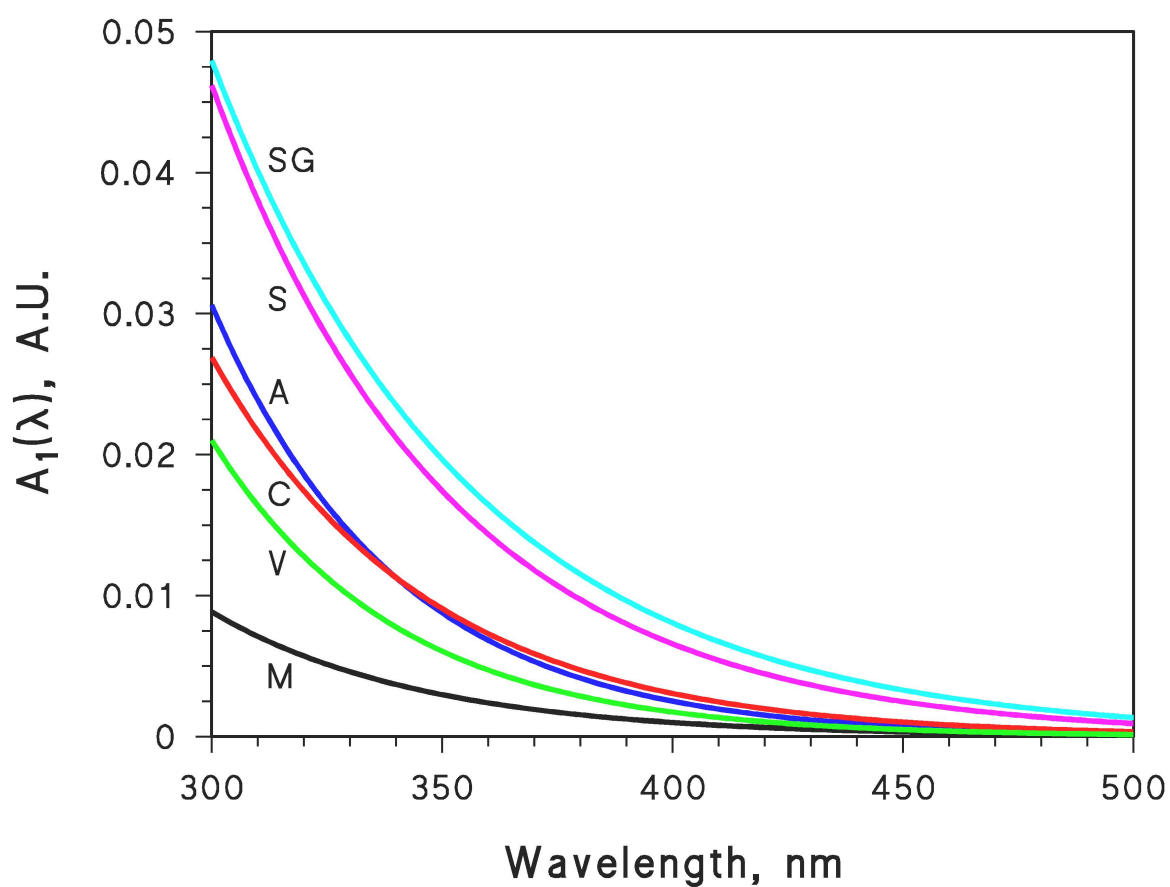


**Figure 1.** Absorption spectra of the irradiated natural water samples. Note that the reported data are referred to an optical path length  $b = 1$  cm, although the actual spectra were measured with a cuvette having  $b = 5$  cm. The meaning of the acronyms, here and in the following figures, is as follows: M = Lago Maggiore (lake), V = Lago di Viverone (lake), C = Lago di Candia (lake), A = Lago di Avigliana (lake), S = Santhià (paddy field), SG = San Germano Vercellese (paddy field).

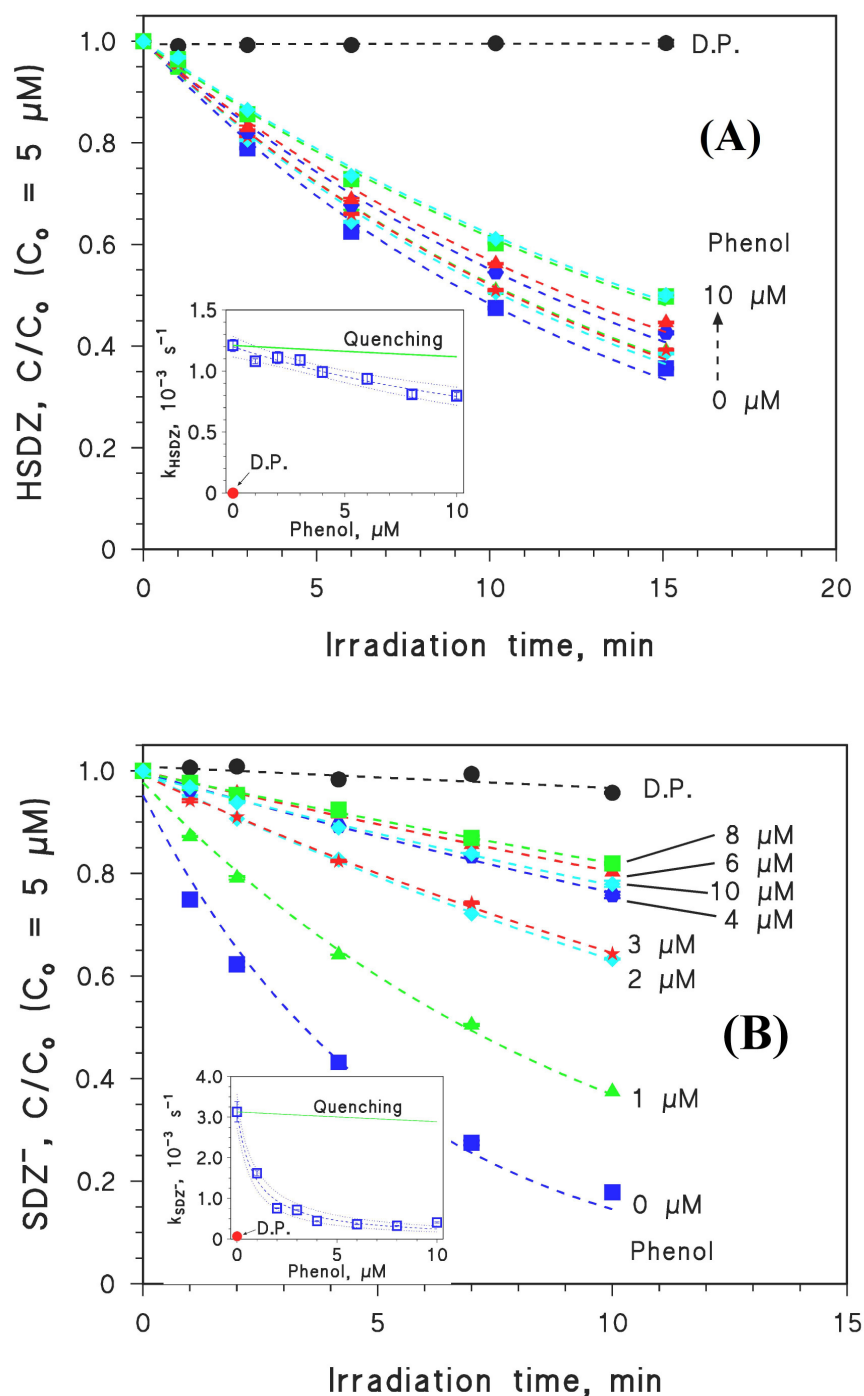


**Figure 2.** (A) Time trend of 5  $\mu\text{M}$  SDZ at pH 5.5 (HSDZ) in the presence of 40  $\mu\text{M}$  CBBP and different concentration values of phenol, with 5 mM phosphate buffer. The data labeled as D.P. are referred to a direct photolysis experiment (5  $\mu\text{M}$  SDZ alone, without CBBP or phenol). The mono-exponential decay fit is given by the dashed curves. The insert in the figure represents the pseudo-first order rate constant of SDZ photodegradation, as a function of phenol concentration, as well as the expected trend if phenol only acted as a quencher of <sup>3</sup>CBBP\*. The dashed curve is the fit of the rate constant data with equation (3), the dotted curves are the 95% confidence bands of the fit. The error bars represent the reproducibility (standard errors) of different injections (concentration values), or the goodness of the fit with a first order kinetics (rate constant data). (B) Same as before, but at pH 8.5 (SDZ<sup>-</sup>).

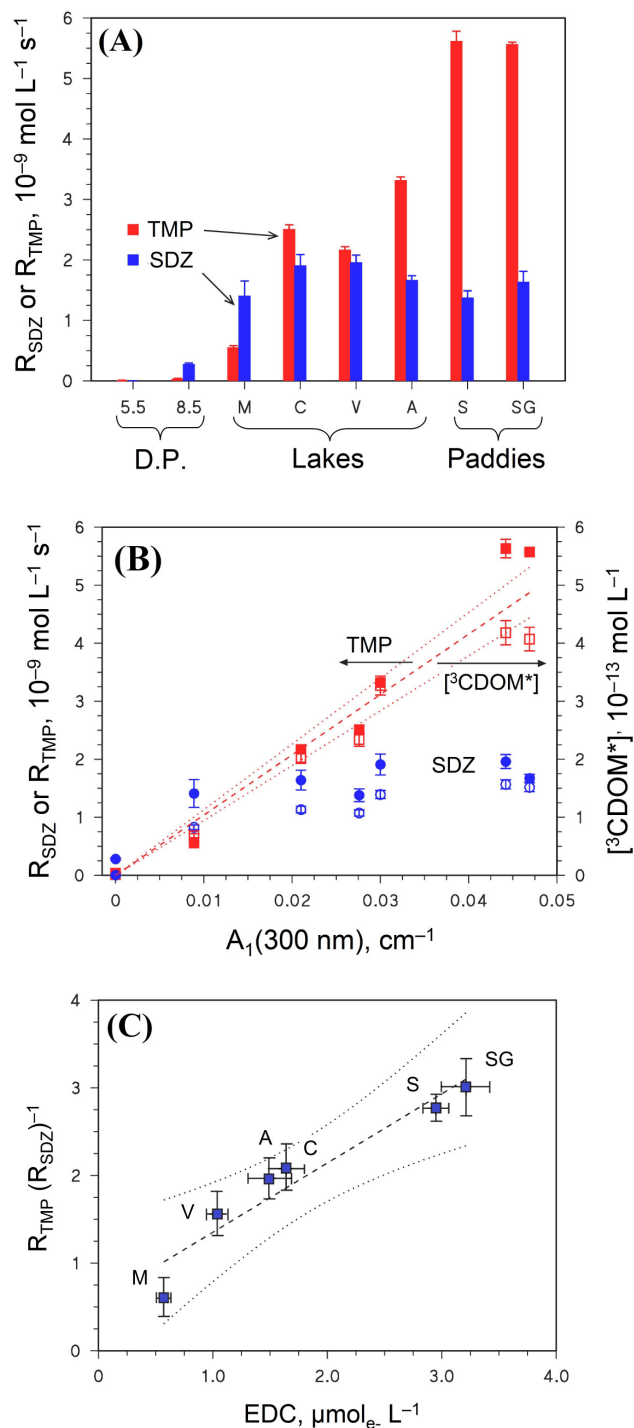


**Figure 3.** (A) Initial degradation rates of  $5 \mu\text{M}$  TMP and  $5 \mu\text{M}$  SDZ, spiked separately to the studied natural water samples (see the caption of Figure 1 for sample acronyms), and added to ultra-pure water at pH 5.5 (prevalence of HSDZ) and 8.5 (prevalence of SDZ<sup>-</sup>). Undissociated TMP prevails at both pH values. The error bars (standard errors) represent the quality of the fit of the experimental concentration data. D.P. = direct photolysis. (B) Same rates as before (solid symbols), as a function of the 300-nm sample absorbance ( $b = 1 \text{ cm}$ ; squares = TMP; circles = SDZ). The results of a second set of experiments are reported as open symbols. Because the TMP rates are directly proportional to  $[^3\text{CDOM}^*]$ , calculated values for  $[^3\text{CDOM}^*]$  are reported in the right Y-axis. (C) Correlation plot between the TMP/SDZ rate ratio ( $R_{\text{TMP}}(R_{\text{SDZ}})^{-1}$ , as average values of the two sets of experimental data reported in panel (B)), and the electron-donating capacity (EDC) of the natural water samples.

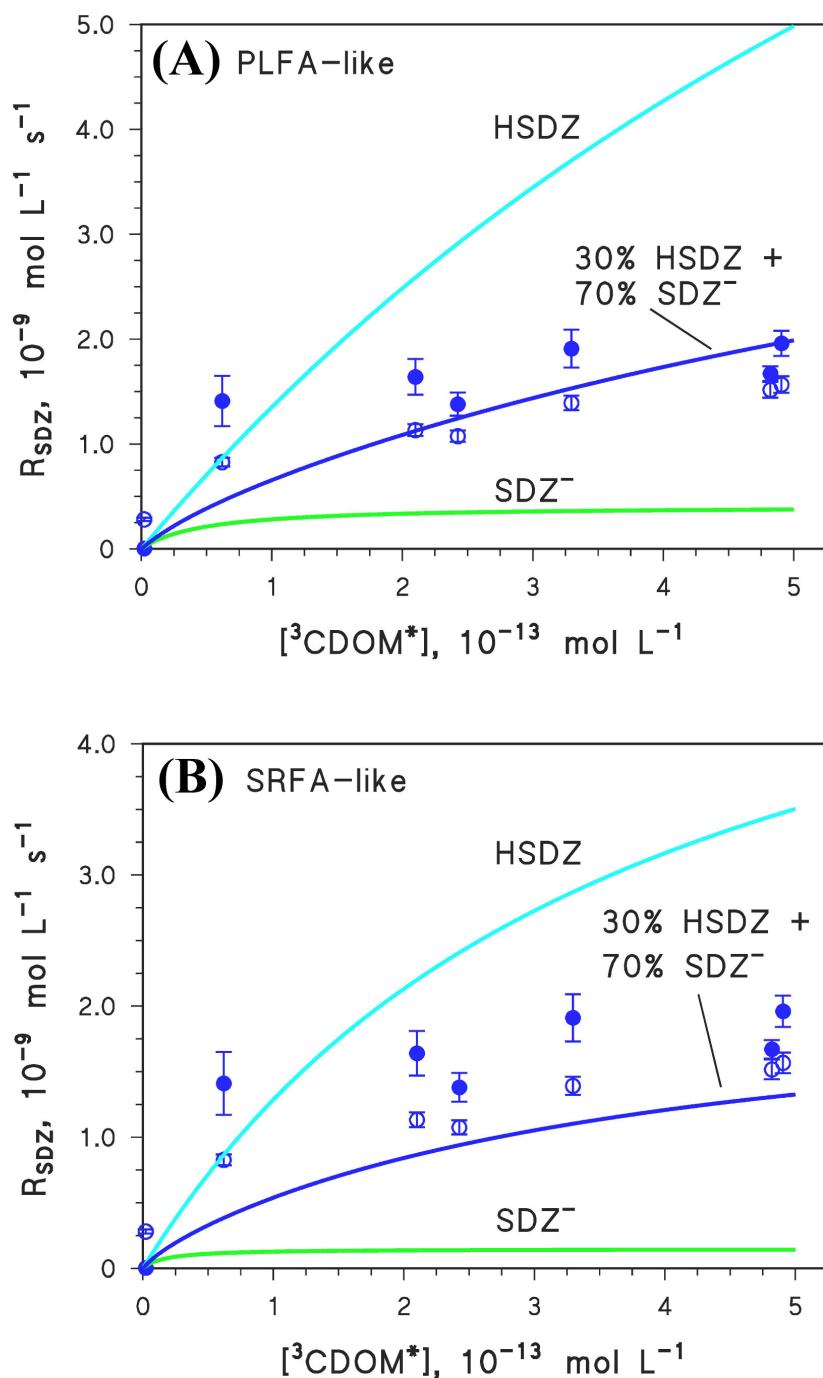


**Figure 4.** (A) Experimental data of  $R_{SDZ}$ , plotted as a function of  $[^3CDOM^*]$ . They are the same  $R_{SDZ}$  values of Figure 3b, with the same meaning of the open and solid symbols (experimental replicas). The values of  $[^3CDOM^*]$  for the experimental points were obtained from  $R_{TMP}$  (Figure 3b), as averages of experimental replicas, with the equation  $[^3CDOM^*] = R_{TMP} / ([TMP] \times (3 \times 10^9 \text{ M}^{-1} \text{ s}^{-1}))$ . The model predictions for the phototransformation kinetics of HSDZ, SDZ<sup>-</sup>, and a mixture of HSDZ + SDZ<sup>-</sup> (pH~7) are also reported for the PLFA-like scenario. The sunlight irradiance of the model was varied, to obtain  $[^3CDOM^*] = 5 \times 10^{-13} \text{ M}$  for  $DOC = 10 \text{ mgC L}^{-1}$  and  $d = 0.01 \text{ m}$ . Because of low water depth, it was  $[^3CDOM^*] \propto DOC$ . (B) Same as before, but the model predictions are referred to the SRFA-like scenario.

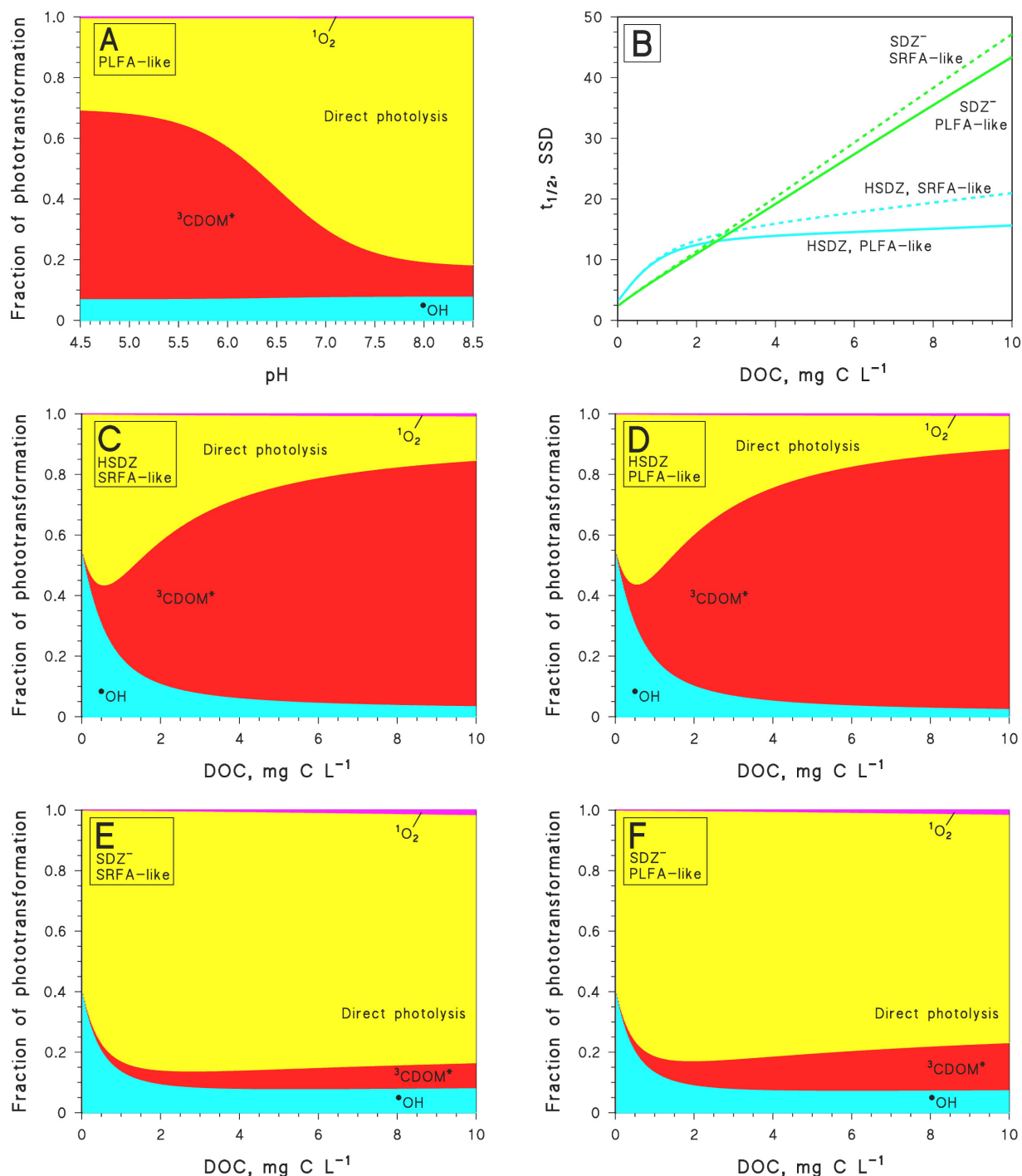


**Figure 5.** (A) Modeled fractions of SDZ transformation *via* different photoreaction pathways, as a function of pH in the PLFA-like scenario (the SRFA-like scenario was almost identical). DOC = 3 mg C L<sup>-1</sup>, *d* = 5 m. (B) Modeled half-lives of HSDZ and SDZ<sup>-</sup> as a function of the DOC, in the SRFA-like and PLFA-like scenarios, for *d* = 5 m. The other plots report the modeled fractions of SDZ transformation *via* different photoreaction pathways, as a function of the DOC, for *d* = 5 m. (C) HSDZ, SRFA-like scenario; (D) HSDZ, PLFA-like scenario; (E) SDZ<sup>-</sup>, SRFA-like scenario; (F) SDZ<sup>-</sup>, PLFA-like scenario. Other water conditions in all the cases were 0.1 mM nitrate, 1 μM nitrite, and 1 mM inorganic carbon.